OPTIMIZATION OF A SOLAR COOLING SYSTEM OPERATING IN FIVE EXPERIMENTAL SCENARIOS

Fernando Palacín[1,2], Carlos Monné [2], Sergio Alonso[2]

[1] Bioclimatic Architecture Department, National Renewable Energy Centre (CENER), C/ Ciudad de la Innovación n_ 7, 31621 Sarriguren, Spain.

[2] Department of Mechanical Engineering, Group of Thermal Engineering and Energy Systems (GITSE), Aragon Institute of Engineering Research (I3A), University of Zaragoza, C/María de luna s/n 50018, Zaragoza, Spain.

1. Introduction

In recent years, the final energy demand of air conditioning systems has increased considerably. The economic prosperity of the last decade and the increase in average seasonal temperatures have prompted the installation of compressor cooling systems powered by electric energy. This has resulted in serious shortages in the electricity supply in urban areas during peak summer temperatures, as well as negative consequences to the environment.

One of the alternatives for these conventional cooling systems are the thermally-fed absorption cooling cycles. These systems are now starting to be installed in the building sector, in combination with solar thermal systems. This synergy is very interesting, given the fact that the period when the solar resource is most available usually coincides with the maximum values of cooling demand. However, for large scale application in buildings, it is necessary to reduce or eliminate several economic, technological and knowledge barriers. This paper is focused in the latter.

There are numerous theoretical studies based on simulation analyses of these types of solar systems but there are insufficient studies providing information about their experimental operation.

This paper presents the conclusions of an analysis of energy performance of the solar-powered absorption cooling system installed at the University of Zaragoza in 2007. The solar cooling system, properly monitored, has operated under five different scenarios since 2007.

The system was installed to resolve the overheating problems of an existing solar thermal system designed to provide domestic hot water. In order to study the performance of the installation, a series of analysis methodologies had to be developed to determine the energy behaviour of this system, both quantitatively as well as qualitatively.

The solar cooling system has been operated under five different experimental scenarios. Initially, the solar cooling installation consisted of 20 m^2 of flat plate collectors, a 4.5 kW, single effect, LiBr-H_2O rotary absorption chiller and a dry cooling tower.

Since then several modifications have been made to the system in order to improve its performance.

The solar field surface of the system, the rotary drum speed of the absorption chiller or geothermal heat rejection system have been, among other issues, the modifications made to the solar cooling system. These modifications were made as result of evaluations made of each scenario.

2. Description of the installation

The installation (Fig. 1.) is located in the sports centre of the University of Zaragoza (Spain). The building contains a sport pavilion, offices, dressing rooms and a gymnasium. The solar cooling installation was designed to resolve the overheating of an existing solar thermal system, which was installed to provide domestic hot water demand of the building. The chilled water produced by the absorption cycle is used to improve the temperature within the gymnasium. The main components of the system are described below.

The solar collector field of the solar cooling installation is divided into arrays. Each array contains 3, 5 and 7 collectors of 2.5 m^2 respectively. Initially only 20m^2 were used to thermally feed the absorption chiller. After preliminary analysis, the solar field area was increased and a 37.5 m^2 field was used to more adequately supply heat to the chiller.

The installation includes a 700 liter hot water tank and an auxiliary boiler but both devices haven't been used, therefore, the absorption chiller will only work when the solar field is able to provide sufficient energy.

A 4.5 kW commercial Rotartica (Schroeder, 2000), single effect, LiBr-H_2O absorption chiller has been used to cool the gymnasium. It has a rotary drum in which the single effect absorption cycle is carried out with the drum rotating at 400 rpm. The rotation favours mass and heat transfers. Inside the drum are the evaporator, the condenser and, instead of a traditional compressor fed with electricity, there are both a chemical absorber and a generator which reduce electrical consumption.

To cool the gymnasium, two fan coils with 6.21 kW of chilling power transfer the chilled water from the evaporator of the absorption machine, thus reducing the ambient temperature.

The initial heat rejection system is a dry cooling tower, which evacuates the waste heat from the condenser and the absorber of the chiller to the exterior of the building. Although the COP would be larger with a wet cooling tower, a dry cooling tower was selected in order to reduce the likelihood of legionella in the humid environment within the wet cooling towers.

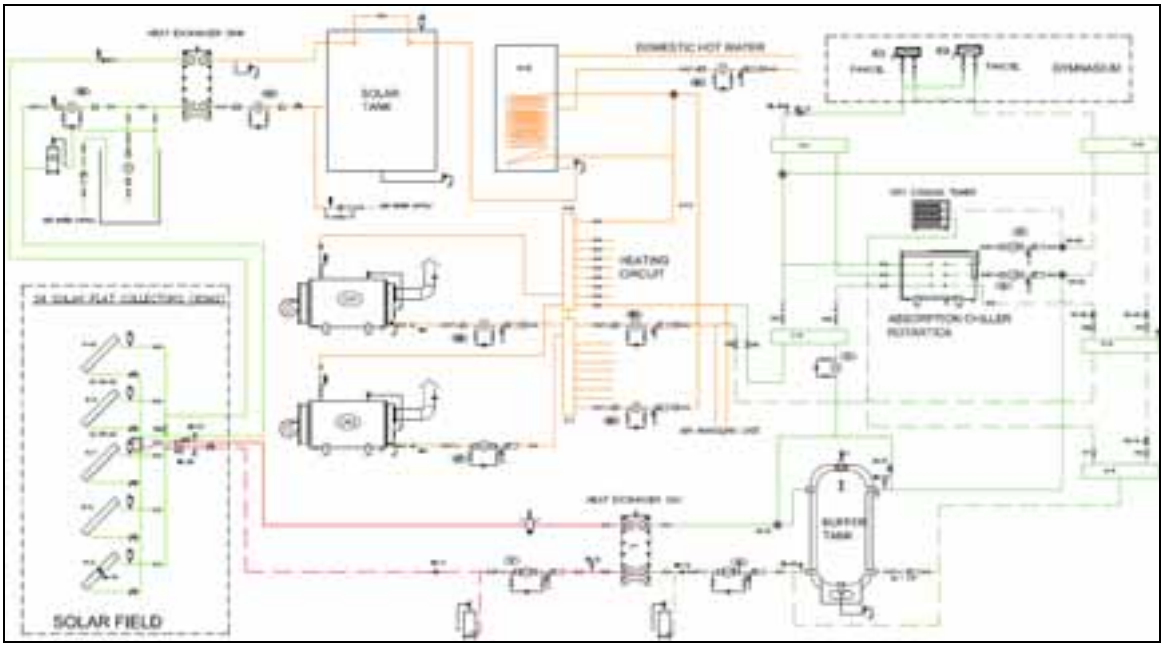

Fig. 1: Initial solar cooling installation scheme

After analyzing the first two scenarios, where the chiller operated with a dry cooling tower, an open geothermal heat rejection system was installed. In this way, as a water well exists near the sport centre building, it was decided to use a geothermal system using this water well because the chiller would be able to operate at a constant temperature in the heat rejection sink (Monne et al., 2011).

From measurements taken in nearby wells, the water temperature was estimated to be approximately 17 ºC. This well water feeds a 25 m^3 water tank, in which the heat produced in the absorption cycle, is rejected. The well is also used to water the athletic fields surrounding the solar cooling installation in summer. This use means the water in the tank is renewed daily. As such, the water temperature is constant, eliminating any potential problems of thermal saturation in the well (Palacín et al, 2010).

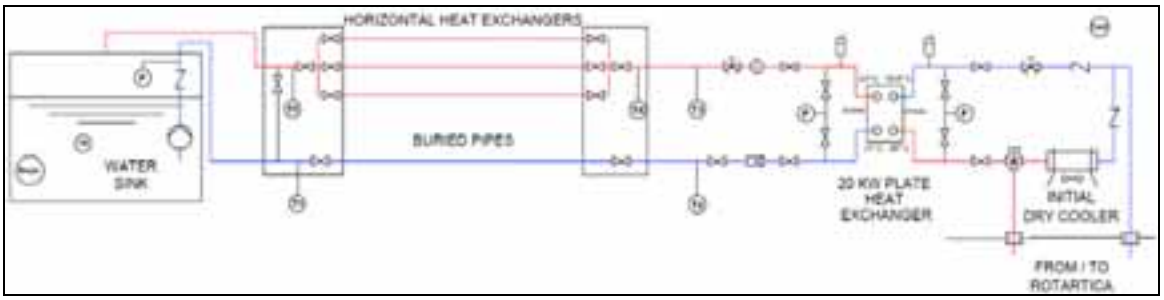

Fig. 2: Geothermal heat rejection scheme

The installation is completely monitored. The procedure of the implementation of the monitoring system was designed to carry out the energy balances of the different components of the installation (Pérez de Viñaspre et al., 2003). There is a PLC unit and a web controller which compose the controlling and value recording system. The monitoring system consists mainly of temperatures sensors and flow meters located in the three water flows that enter the absorption machine. Two temperature sensors (close to the absorber and the condenser of the absorption machine) measure the inlet ($T_{c,i}$) and outlet ($T_{c,o}$) temperature of the flow between the absorption chiller and heat rejection system. Two more temperature sensors measure the inlet ($T_{ch,o}$) and outlet ($T_{ch,o}$) temperature of the flow between the absorption chiller and the fan coils (the measure is taken near the evaporator in the absorption machine). Two temperature sensors measure the inlet ($T_{g,i}$) and outlet ($T_{g,o}$) temperature of the flow between the absorption chiller and the heat exchanger (the measure is taken near to the generator in the absorption machine). Furthermore, there is a flow meter in each one of these loops; the water flow that goes to the generator (m_g), to the fan coils (m_{ch}) and to the heat rejection system (m_c).

In addition, there are dry bulb outdoor temperature, humidity, and radiation sensors, flow meters and energy meters placed throughout the installation. As such, the outdoor and indoor conditions of the installation are well defined.

3. Methodology of analysis

To analyze the results of the experimental solar cooling system installation, a novel methodology was created based on the consulted bibliography (Izquierdo et al., 2007). Four different types of graphics were prepared in order to compare and relate variables: 'Rank Graphics', 'Phase Graphics', 'Stationary Graphics' and 'Trend Graphics'(Monné et al., 2008).

'Rank Graphics'. These graphics represent the evolution versus time of all the days that were studied, of the following variables: the generator circuit flow rate (m_g), the fan coils circuit flow rate (m_{ch}), the finned tube heat exchanger circuit flow rate (m_{ch}), the inlet and outlet temperature at the generator (T_{ig}, T_{og}), the inlet and outlet temperature at the evaporator ($T_{ch,i}$,$T_{ch,o}$), the inlet and outlet temperature in the flow from the heat rejection system ($T_{c,i}$, $T_{c,o}$), the irradiation (I), the coefficient of performance (COP), the power transferred in the generator (W_g), the power transferred in the evaporator (W_{ch}) and the power transferred in the condenser and the absorber (W_c). By analyzing these variables of the installation, it is possible to comprehend the overall performance of the rotary absorption system (Fig. 5).

'Phase Graphics'. There are three different graphics for each day. The first represents $T_{g,i}$, $T_{g,o}$, $T_{ch,o}$, $T_{ch,o}$, $T_{c,i}$, $T_{c,o}$, I and T_{dbo} evolution versus time, the second reflects m_c, m_{ch}, m_g, development versus time and the third one shows COP, W_g, W_{ch} and W_c evolution versus time. The influence of some variables on the others is shown in this type of graphics.

'Stationary Graphics'. To compare the performance of the absorption chiller on different days, it is necessary to define the stationary period, in which the chiller works in a stationary situation. This period of time is defined as an interval of time. For each day studied, the minimum T_{oev} is recognized, and the interval of time of the steady situation defined. The points inside this interval will be those which do not differ more than 5%

from the minimum $T_{ch,o}$ ($[(T_{ch,o})_{min}$, $1.05*(T_{ch,o})_{min}]$). The stationary interval is usually found in the central part of the temporary representation, and the values placed in the stationary period represent a stable behaviour in the performance of the chiller. The stationary values will form the base of the analysis (Ausdurbali et al., 2003), (Martinez et al., 2009).

'Trend Graphics'. For this type of graphic, a calculation of the average values of all the parameters analyzed in the stationary time, of all the days studied, has to be made. Afterwards, each of the variables is charted with the other ones, on different graphics. The average values follow the same evolution as the temporary values, and the trend lines are overlapped. Consequently, average values can be considered representative values of the temporary ones. With the average values, an average performance of the installation can be calculated.

The results and the conclusions of this work are reached based on the Trend Graphics.

4. Definition of the experimental scenarios

With the aim of optimizing and improving the performance of the absorption chiller, several modifications to the original installation built in 2007 were made. Because of these modifications the chiller performance has been analyzed under five different scenarios:

a) Scenario 1:

In the summer of 2007 the solar cooling system began operating with the following features:

- Solar field surface area: 20 m^2
- Rotary drum speed: 300 rpm.
- Heat rejection system: Dry cooling tower

b) Scenario 2

The analysis of the first results of the scenario 1 highlighted the need of increase the solar field surface area because the initial field was insufficient to properly feed the absorption chiller. Using the modularity capacity of the solar field, another array of five collectors was added, resulting in the following:

- Solar field surface area: 37.5 m^2
- Rotary drum speed: 300 rpm.
- Heat rejection system: Dry cooling tower

c) Scenario 3

After a regular maintenance operation, the speed of the rotary drum of the chiller was increased to 400 rpm, the rest of the main parameters of the installation being equal.

- Solar field surface area: 37.5 m^2
- Rotary drum speed: 400 rpm.
- Heat rejection system: Dry cooling tower

d) Scenario 4

The most important conclusion reached as result of the analysis of the first three scenarios was the negative influence of the outdoor temperature on the COP, given that the heat rejection system used was a dry cooling tower. For this reason, the 25 m^3 water well was harnessed as the heat rejection system of the installation.

- Solar field surface area: 37.5 m^2
- Rotary drum speed: 400 rpm.
- Heat rejection system: Geothermal system
- Geothermal flow: 0.71 litre$\cdot s^{-1}$

e) Scenario 5

Unfortunately the well water temperature during its operation was not 17ºC, as was found in nearby wells. The mean well water temperature was 25ºC, implying that the heat exchanger placed between the absorption chiller and the geothermal system had to be redesigned. Meanwhile, the geothermal flow value was increased up to 95 l/min in order to step up the heat exchange in the flat heat exchanger.

- Solar field surface area: 37.5 m^2
- Rotary drum speed: 400 rpm.
- Heat rejection system: Geothermal system
- Geothermal flow: 1.58 litre·s^{-1}

5. Energy results of the scenarios

The results methodology explained in point 3, was applied to the entirety of results obtained from the monitored system of the installation. Although the different types of graphics provide important information about the performance of the chiller and the solar cooling system, the conclusions and the energy results are based solely on the phase and trends graphics.

Using the phase range (Figure 3) the temperatures of a typical operation day of the chiller can be determined. The chiller engages automatically when the inlet temperature of the generator reaches 80 ºC. At this point the absorption chiller provides cooling energy by means of the evaporator. The outlet temperature of the evaporator reaches values of approximately 10 ºC. According to the heat rejection system, the initial values at the beginning of the day are between 30 ºC – 35 ºC, however, due to the inlet temperature of the generator and the fact the outdoor temperature increases afternoon, the dry cooling tower cannot maintain the rejection capacity. As result, the temperatures of this loop increases, too.

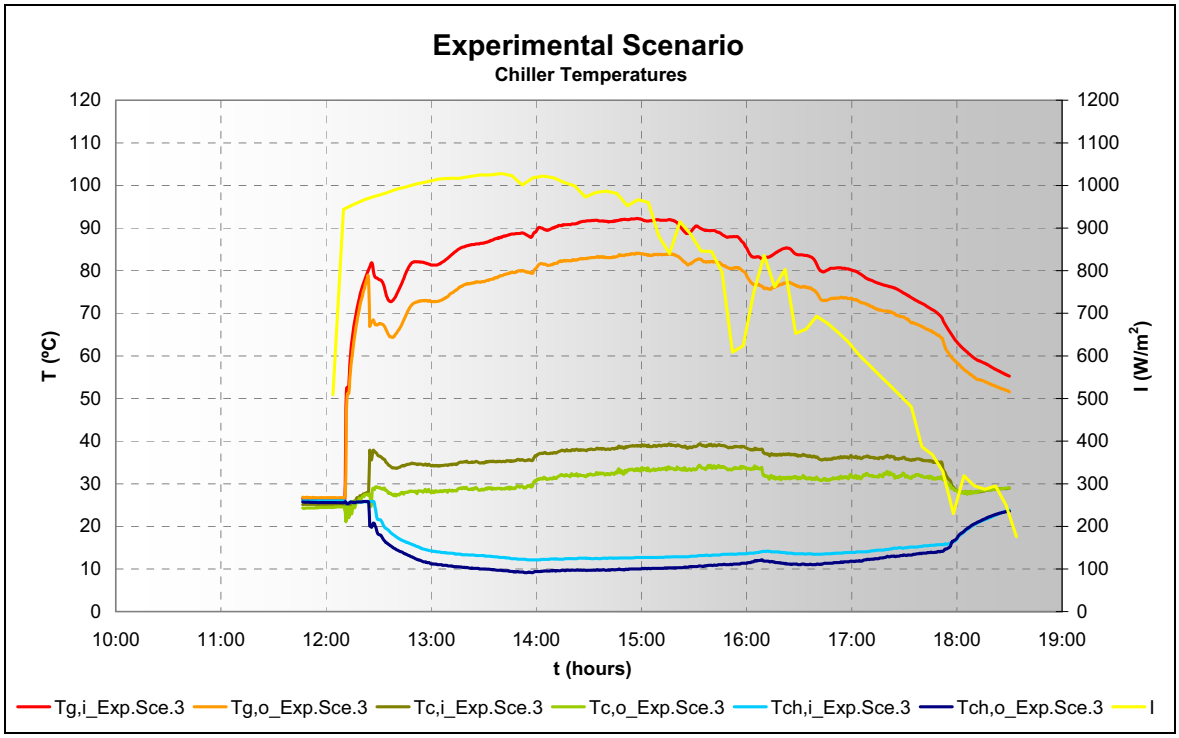

Fig. 3: Typical day of the performance of the chiller (Temperatures)

This fact is clearly shown in Figure 4 where the capacities and the COP of the chiller are shown. The best results of the capacities and the COP of the chiller are shown between the 1 p.m and 2 p.m. when,, although the generator temperature value does not exhibit the highest values of the day, due to the heat rejection system operating properly, the chilled capacity and the COP values are at their optimum values. Then, as the day progresses, the capacities fall in spite of a higher solar thermal availability in the generator of the chiller.

The main objective of this paper is to examine how the modifications made to the installation affected chiller performance. To carry out this examination of the performance throughout the various scenarios, trends graphics were used.

a) Influence of the solar field surface area

The operational difference between scenario 1 and 2 is the size of solar field surface area. Whereas in the first scenario the ratio between the surface and the cooling capacity of the chiller is 4.44 m^2/kW in the second one this ratio increases up to 7.44 m^2/kW.

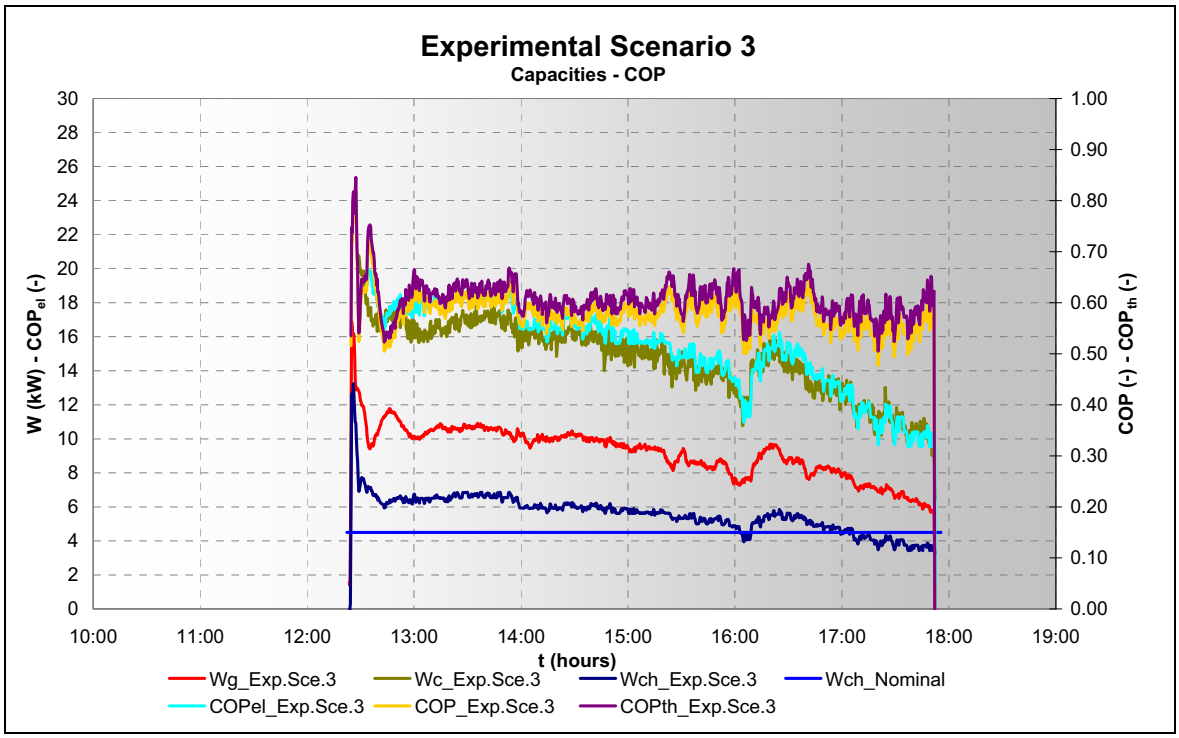

Fig. 4: Typical day of the performance of the chiller (Capacities - COP)

Figure 5 shows capacities and the COP of the chiller operating in both scenarios. As can be seen in the figure, the solar field is incapable of thermally feeding the chiller generator. On the other hand, the optimal input temperature of the chiller is approximately 91 ºC. From this point the absorption machine gives out less capacity and COP. This temperature coincides with the manufacturer's recommendation.

These results indicate that the usual pre-design value for this ratio (3 m^2/kW) is insufficient for the design of the solar field. In this case the solar cooling system works suitably with higher ratios. As result, other researchers have proposed ratios over 8.5 m^2/kW (Izquierdo et al., 2007).

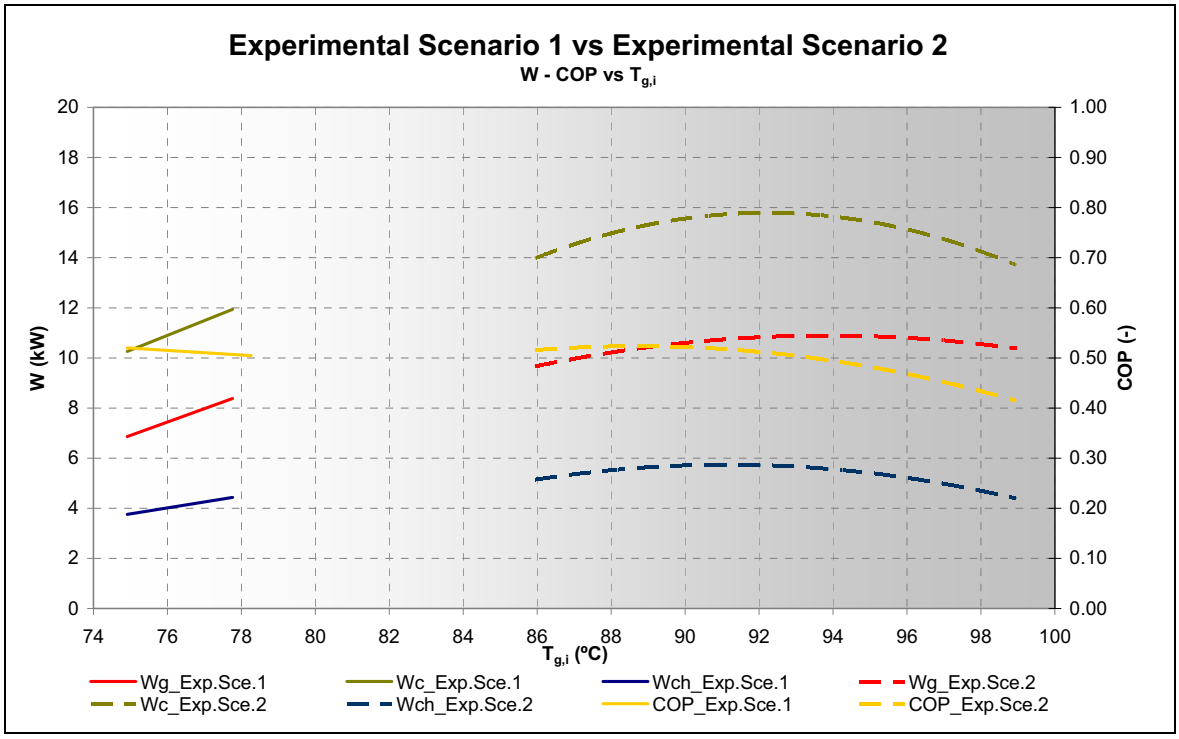

Fig. 5: Influence of the solar field surface area

b) Influence of the rotary speed of the absorption drum

As it was mentioned before, the original rotary speed of the absorption process drum was 300 rpm. Nevertheless during regular maintenance,, this speed was increased to 400 rpm. As shown in Figure 6, this resulted in an increase of the capacities of the chiller. The machine produces more chilling capacity with less heat, so that the COP generates better values in the third scenario than in the first two.

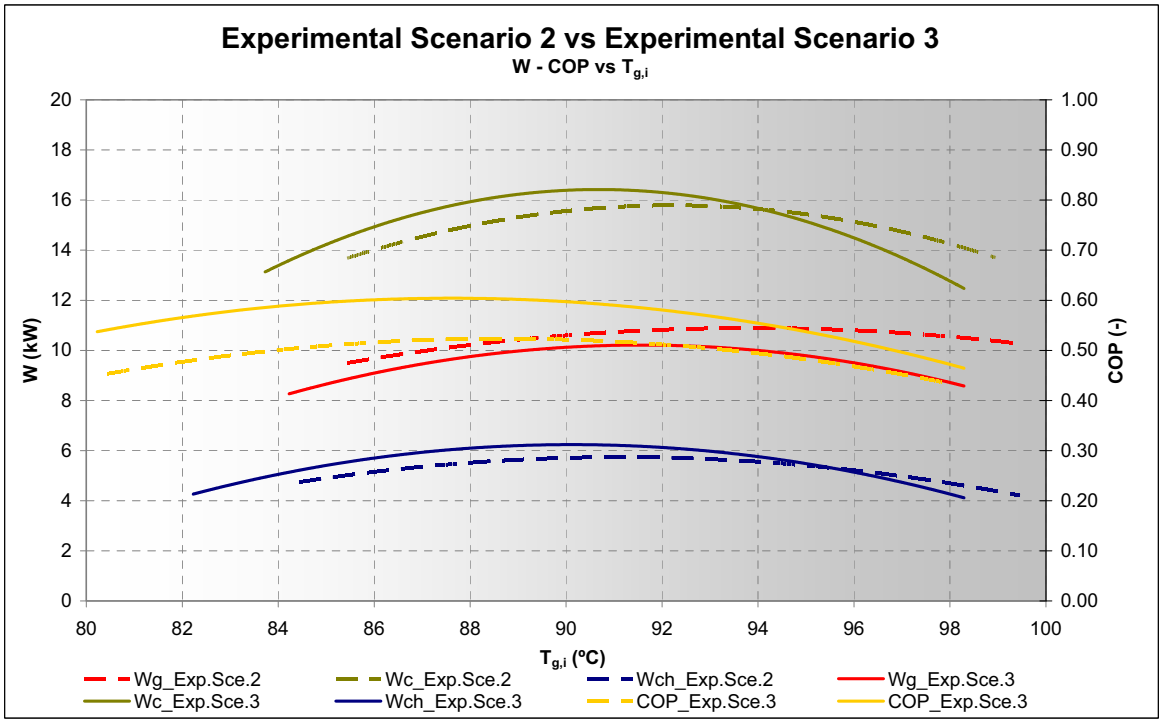

Fig. 6: Influence of the rotary drum speed

c) Influence of heat rejection system

One of the main problems of cooling systems is the influence of the heat rejection system on the performance of the thermodynamics cycle. Figure 7 shows the results of this influence on the performance of the Rotartica during the first two years of operation.

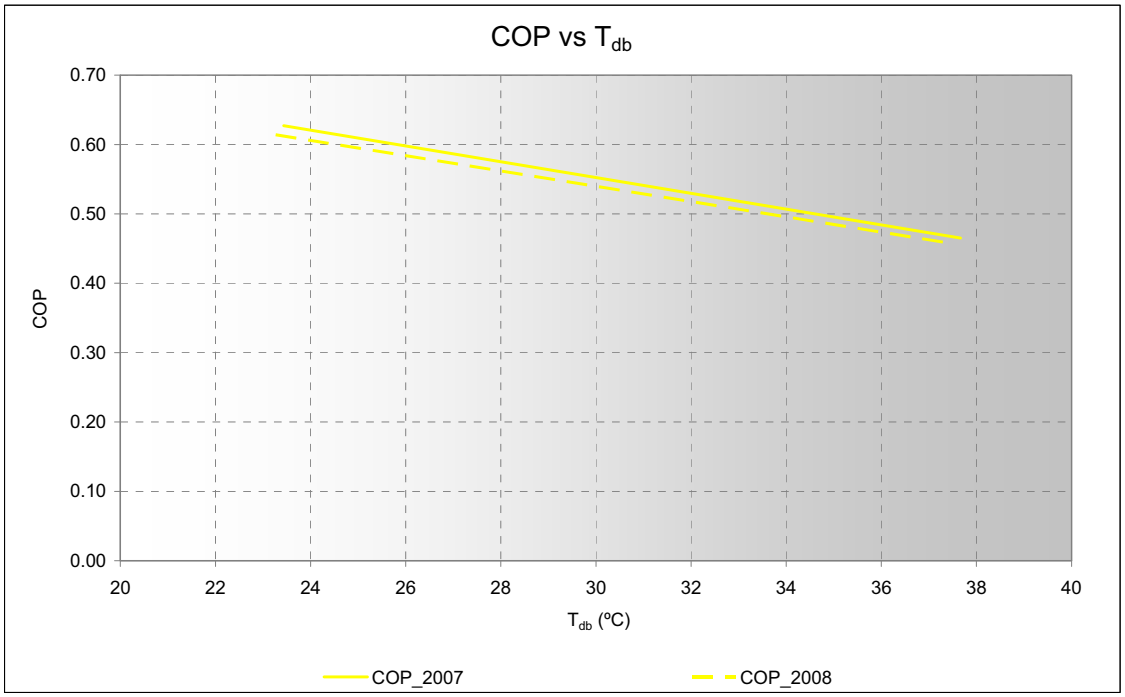

Fig. 7: Influence of the outdoor temperature on the COP of the chiller

Figure 7 shows the negative influence of the outdoor temperature on the COP of the chiller. In 2009, to mitigate this situation, the solar cooling installation began operating with a new geothermal heat rejection system. The effect of this heat rejection system it can be seen on Figure 8

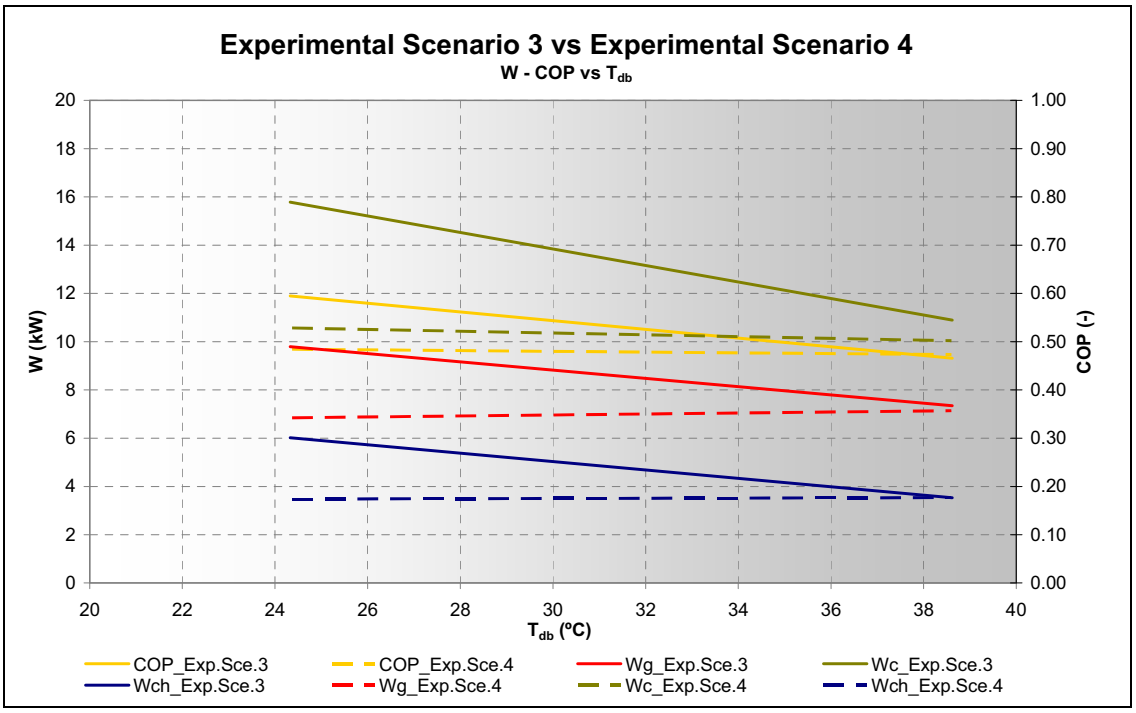

Fig. 8: Influence of the heat rejection system

The COP and the chiller capacities maintain values constant when the outdoor temperature increases, so the negative influence of this temperature is offset.

d) Influence of geothermal heat rejection system flow

Although with the use of the geothermal system the chiller performance operates with more stable values, these values do not reach the nominal values of the chiller.

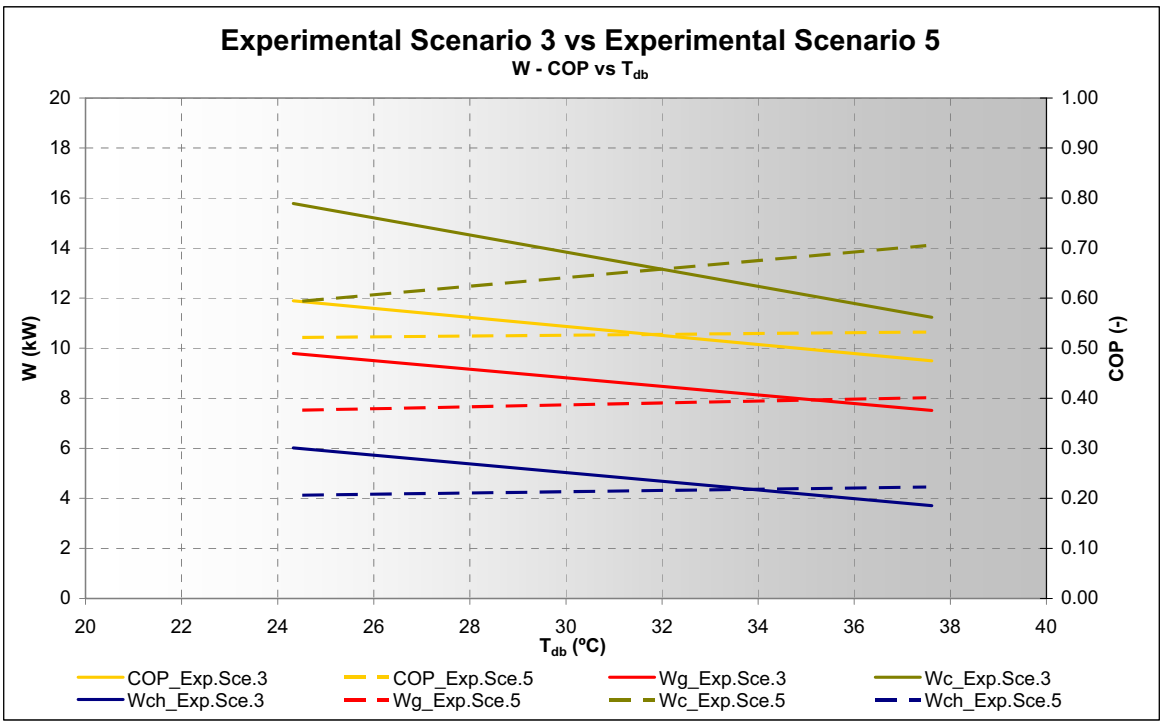

Fig. 9: Influence of the heat rejection system flow

This fact is, as was explained in point 4, due to the operational temperature of the water well. In the design phase this temperature was set to 17 ºC. However, in the first month of operation, this temperature was actually found to be 25 ºC. As such, the flat heat exchanger had to be redesigned according to the operational temperature of the well. The solution adopted to increase the performance of the chiller was to increase the geothermal flow from 0.71 litre·s^{-1} to 1.58 litre·s^{-1}. The results of this modification are showed in Figure 9.

Figure 9 also shows the chilling capacity and the COP of the chiller when operated with the initial dry cooler system and then with the new flow in the geothermal system. As can been seen in the figure, when the outdoor temperature is below 33 - 34 ºC, the chilling capacity and the COP of the absorption chiller is greater when it operates with the dry cooler, although the chilling capacity shows constant values in the case of operation with the geothermal system. At this point, a hybrid heat rejection system could be implemented in order to optimize the use of the optimal heat rejection sink at every moment (Salgado, 2009).

Lastly, a summary of the main values of the capacities and the COP of the absorption chiller working in the different scenarios is shown in Table 1:

Tab. 1: Results of the absorption chiller capacities operating in the different scenarios

Scenario	W_g (kW)	W_c (kW)	W_{ch} (kW)	COP (-)
Experimental Scenario 1	7.45	11.91	4.02	0.51
Experimental Scenario 2	10.62	16.16	5.38	0.49
Experimental Scenario 3	8.44	15.43	5.78	0.52
Experimental Scenario 4	7.08	10.50	3.5	0.47
Experimental Scenario 5	7.61	12.25	4.18	0.52

The best results obtained of the chiller are found in the experimental scenario 3. This is due to the fact that the solar field size was increased and the rotary drum speed had been previously optimized. On other hand, in this scenario, where the chiller continued to be operated with the dry cooling tower, the outdoor temperature values were lower than the values shown in the first scenarios.

It expected that after the optimization of the flat heat exchanger of the geothermal heat rejection system, the chiller can improve the results of the third scenario, as can be seen in the simulation results carried out with TRNSYS (Palacín et al., 2011), and shown in Figure 10.

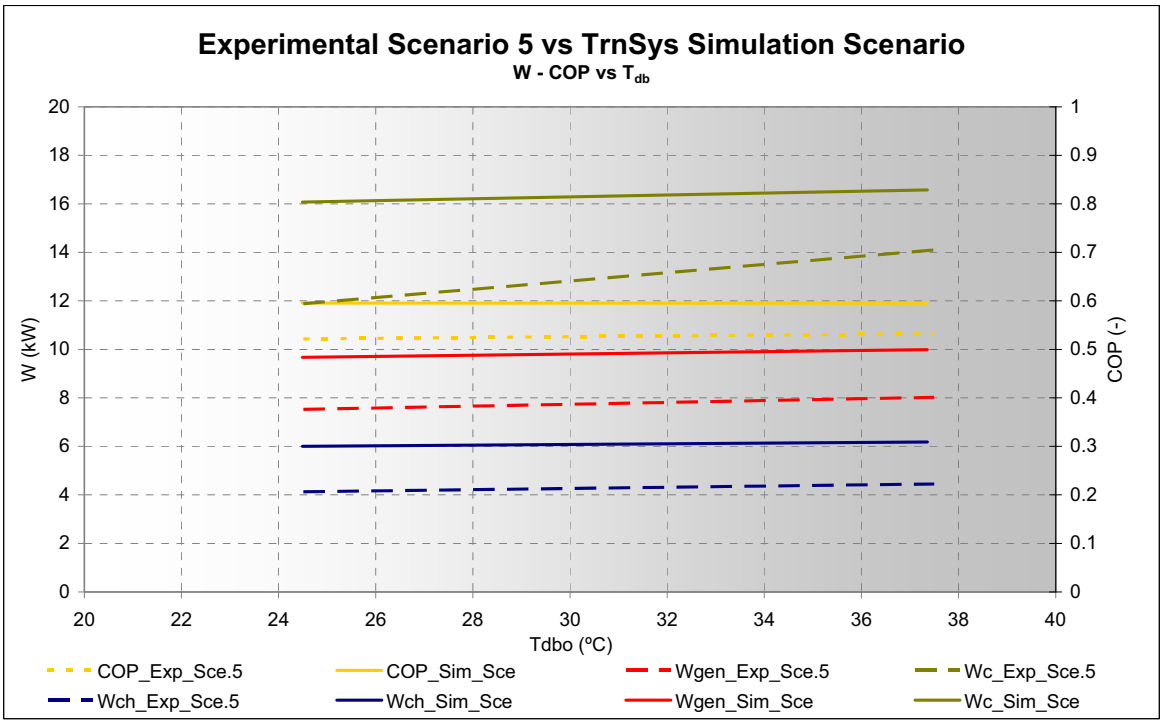

Fig. 10: Expected performance of the chiller operating with the geothermal system

6. Conclusions

In this paper, the results of an experimental solar cooling installation working under five different scenarios of operation have been presented.

In each of these scenarios, a modification to the solar cooling installation was carried out. The solar field size, the rotary speed of the absorption processes, the heat rejection system or its operation flow were modified in order to evaluate the global performance of the absorption chiller.

The first conclusion of the paper has to do with the ratio between the solar field surface size and the cooling power of the chiller. The usual value used to pre-design this kind of system is set to 3 m^2/kW. In the case of the installation presented in this paper, this value is inadequate. The experimental ratio in the installation located in Zaragoza is 8.33 m^2/kW.

The second conclusion is that an increase in the rotary drum speed improves the absorption cycle processes so that the chiller capacities are also improved.

Finally, the use of a geothermal heat rejection system eliminates the known problem of the cooling system as the negative influence of the ambient temperature on the COP of the chiller. Nevertheless, because of the operational temperature of the well water is higher than originally calculated, the flat exchanger of the heat rejection loop has to be redesigned.

In addition, as the initial heat rejection system, the dry cooling tower, was not removed from the installation, a hybrid heat rejection system could be implemented on the solar cooling system in order to optimize its heat rejection capacity.

7. References

http://andyschroder.com/rotartica.html

Asdrubali, F.; Baldinelli, G.; Presciutti, A., 2009. An experimental solar cooling system with a small size absorption chiller: Design and first measurement. 3rd International Conference Solar Air-Conditioning. Actas del congreso, 430-435. 30th September to 2nd October 2009. Palermo (Italia).

Izquierdo, M.; Lizarte, R.; Marcos, J.; Gutiérrez, G., 2007. Air conditioning using a single effect lithium bromide absorption chiller: Results of a trial conducted in Madrid in August 2005 Applied Thermal Engineering, 28, 1074-1081.

Martínez, P. J.; García, A.; Pinazo, J. M., 2003. Performance analysis of an air conditioning system driven by natural gas. Energy and Buildings, 35, 669-674.

Monné, C.; Alonso, S.; Palacín, F.; Serra, L., (2011). "Monitoring and simulation of an existing solar powered absorption cooling system in Zaragoza (Spain)". Applied Thermal Engineering, 31, 28 - 35. doi:10.1016/j.applthermaleng.2010.08.002.

Monné, C.; Guallar, J.; Alonso, S.; Palacín, F., (2008). Instalación Experimental De Refrigeración Solar - Primeros Resultados. XIV Congreso Ibérico y IX Congreso Iberoamericano de Energía Solar. Actas del congreso, pp. 315-320. 17-21 junio, 2008. Vigo.

Palacín, F.; Monné, C.; Alonso, S., (2010). Mejora experimental del comportamiento dinámico de una instalación de refrigeración solar por absorción optimizando su sistema de disipación. I Congreso sobre Arquitectura Bioclimática y Frío solar (PSE-ARFRISOL). Actas del congreso, pp. 71. 23 al 26 de Marzo. Roquetas de Mar (Almería).

Palacín, F.; Monné, C.; Alonso, S., (2011). "Improvement of an existing solar powered absorption cooling system by means of dynamic simulation and experimental diagnosis". Energy, 36, 4109 - 4118 doi:10.1016/j.energy.2011.04.035.

Pérez de Viñaspre, M.; Bourouis, M.; Coronas, A.; García, A.; Soto, V.; Pinazo, J. M., (2004). Monitoring and Analysis of an Absorption Air-Conditioning System. Energy and Buildings, vol. pp. 933-943.

Salgado, R.; Burguete, A.; Rodriguez, M. C.; Rodriguez, P., (2008). Simulation of Absorption Based Solar Cooling Facility Using a Geothermal Sink for Heat Rejection. EUROSUN 2008. 7 - 10 Octubre 2008. Lisboa.